



# A FSO-NOMA Communication System with Málaga Turbulence and Non-Zero Boresight Pointing Error for 6G Applications

Prakriti Saxena<sup>\*</sup>, Yeon Ho Chung<sup>#</sup>

*Artificial Intelligence Research Center, Pukyong National University, Busan, 48513, Republic of Korea*

*Department of Information and Communications, Pukyong National University, Busan, 48513, Republic of Korea*

*Email: <sup>\*</sup>[prakritisaxena@pknu.ac.kr](mailto:prakritisaxena@pknu.ac.kr), <sup>#</sup>[yhchung@pknu.ac.kr](mailto:yhchung@pknu.ac.kr)*

*Corresponding author: Yeon Ho Chung*

## Abstract

To support the huge data traffic which is expected in 6G communication systems, efficient backhaul techniques are needed to deliver the data traffic of multiple users simultaneously. To achieve this goal, smart multiple access techniques like non-orthogonal multiple access (NOMA) should be studied. In this paper, the ramifications of one-bit feedback based beamforming scheme on multiple-input-single output (MISO) NOMA based free space optical (FSO) communication systems under the combined effects of Málaga ( $\mathcal{M}$ ) turbulence, non-zero boresight pointing error (PE) and successive interference cancellation (SIC) error are evaluated. The feedback is presumed to be error free. It is inferred from the obtained results that the effect of the SIC error is suppressed by using the proposed beamforming scheme. Furthermore, the average bit error rate (BER) performance of all the transmitting antennas are identical.

2018 The Korean Institute of Communications and Information Sciences. Publishing Services by Elsevier B.V. This is an open access article under the CC BY-NC-ND license (<http://creativecommons.org/licenses/by-nc-nd/4.0/>).

**Keywords:** 6G, boresight, free-space optical communications, Málaga distribution, Non-orthogonal multiple access, successive interference cancellation.

## 1. Introduction

The explosive demand of data and bandwidth thirsty applications such as virtual reality (VR), augmented reality (AR) etc. are bound to increase the challenges for next generation 6G wireless communication systems. With the advent of 6G, it is expected that the connectivity will increase by tenfold as compared to 5G communication systems and the data rates are expected to reach 1 Tera-bit per second (Tbps). To meet such high demands, there is a need for highly efficient next generation multiple access techniques such as non-orthogonal multiple access (NOMA) which can be used for efficient backhaul communication. FSO communication is an excellent technology for providing backhaul connectivity in 6G communication systems. Not only are FSO links free to use, they are also immune to the electromagnetic interference caused by RF signals. Features like high bandwidth and interference immunity make FSO link up to 25 times more efficient than an RF link in terms of capacity. It is also a cost-efficient solution compared to optical fiber [1].

In this work, we propose a feedback based beamforming scheme for  $N \times 1$  multiple-input-single output (MISO) NOMA FSO communication systems for 6G applications. The

combined detrimental effects of Málaga ( $\mathcal{M}$ ) distributed atmospheric turbulence, boresight pointing error (PE), and successive interference cancellation (SIC) errors are also taken into consideration for the performance analysis of the considered system.

## 2. Preliminaries

### 2.1 System Description

We consider an  $N \times 1$  FSO MISO system using subcarrier intensity modulation (SIM) binary phase shift keying (BPSK) technique where  $N$  is the total number of transmitters (TXs). Each TX generates a different symbol,  $s_i \in \{1, -1\}$  where  $i \in \{1, 2, \dots, N\}$  and transmits it to the same receiver (RX) in the same time and frequency band. The symbols are not orthogonal to each other. This multiple access technique is called NOMA. A feedback link from the RX transmits a part of the channel state information (CSI) back to the TX side where they will receive information about which TX's channel gain is higher than the other. Based on this information, beamforming weights are then allocated to each TX. The highest weight is assigned to the TX with the highest channel gain and the lowest weight is assigned to the TX with the lowest channel gain. The beamforming vector is given as  $\mathbf{v} = [v_1, v_2, \dots, v_N]^T$  such that  $v_1 > v_2 > \dots > v_N$ ,  $\sum_{t=1}^N v_t \leq N$ , and  $[\cdot]^T$  denotes the transpose operator. This

further increases the difference in path loss of each channel, thereby helping in the SIC technique for decoding each symbol at the RX side [1]. The received signal at the RX is given by:

$$y = \frac{\eta}{N} [I_1 s_1, I_2 s_2, \dots, I_N s_N] [v_1, v_2, \dots, v_N]^T + e, \quad (1)$$

where  $I_i$  represents the real valued channel irradiance of the link between the  $i^{th}$  TX and the RX aperture,  $\eta$  is the optical-to-electrical conversion factor, and  $e$  denotes the additive white Gaussian noise (AWGN) with zero mean and variance  $\sigma^2$ . Further, the FSO channel gain  $I_i = I_a I_p I_l$  consists of three components namely, (i)  $I_a$  which is the atmospheric turbulence (AT) modeled using  $\mathcal{M}$  distribution [3], (ii)  $I_p$  which represents the non-zero boresight pointing error (PE), (iii)  $I_l$  which constitutes the path loss and is a deterministic constant modeled by the Beer-Lambert's law. The probability density function (PDF) of the channel gain under the combined effects of  $\mathcal{M}$  distribution and non-zero boresight PE is given by [4]:

$$f_{I_i}(I_i) = \frac{\psi_{mod}^2 A}{2 I_i} \sum_{k=1}^{\beta} b_k G_{1,3}^{3,0} \left( \frac{\alpha \beta I_i}{(g\beta + \Omega') A_{mod}} \left| \psi_{mod}^2 + 1 \right|, I_j > 0, \right) \quad (2)$$

$$A = \frac{2\alpha^{\alpha/2}}{g^{1+\frac{\alpha}{2}\Gamma(\alpha)}} \left( \frac{g\beta}{g\beta + \Omega'} \right)^{\beta + \alpha/2}, \quad (2a)$$

$$\Omega' = \Omega + 2b_0\rho + 2\sqrt{2b_0\rho} \cos(\phi_a - \phi_b), \quad (2b)$$

$$b_k = \binom{\beta-1}{k-1} \frac{(g\beta + \Omega')^{1-\frac{k}{2}}}{(k-1)! \left( \frac{\alpha\beta}{g\beta + \Omega'} \right)^{\frac{\alpha+k}{2}}} \left( \frac{\Omega'}{\gamma} \right)^{k-1} \left( \frac{\alpha}{\beta} \right)^{\frac{k}{2}}, \quad (2c)$$

where  $\alpha > 0$  is the effective number of large scale cells of the scattering process,  $\beta$  is a natural number which represents the amount of fading,  $i \in \{1, 2, \dots, N\}$ ,  $N$  is the total number of TXs,  $2b_0$  is the average power of total scatter components. The average power of the scattering component received by off-axis eddies is given by  $g = 2b_0(1 - \rho)$ , where  $0 \leq \rho \leq 1$  is the amount of power coupled to the line-of-sight (LOS) component,  $\Omega'$  represents the average power from the coherent component,  $\Omega$  is the average power of the LOS component,  $\phi_a$  and  $\phi_b$  are the deterministic phases of LOS and coupled to LOS scatter term. The beam width is denoted by  $w_z \approx \theta_z$ , where  $\theta$  is divergence angle and  $z$  is the link length between TX and RX,  $v = \frac{\sqrt{\pi}a}{\sqrt{2}w_z}$ ,  $A_0 = [\text{erf}(v)]^2$  is the fraction of the collected power at the center of the RX, and  $a$  is the aperture radius of the detector. Let us denote the boresight along the horizontal and vertical directions by  $\mu_x$  and  $\mu_y$ , respectively, and the corresponding jitter variances by  $\sigma_x^2$  and  $\sigma_y^2$ . An equivalent beam radius at the RX is given by  $w_{zeq}^2 = \frac{w_z^2 \sqrt{\pi} \text{erf}(v)}{2v \exp(v^2)}$ . Moreover,  $\psi_x = \frac{w_{zeq}}{2\sigma_x}$  and  $\psi_y = \frac{w_{zeq}}{2\sigma_y}$  are the ratios of the equivalent beam radius at the RX to the standard deviation with the respective PE displacement at the RX.  $G = \exp \left( \frac{1}{\psi_{mod}^2} - \frac{1}{2\psi_x^2} - \frac{1}{2\psi_y^2} - \frac{\mu_x^2}{2\sigma_x^2\psi_x^2} - \frac{\mu_y^2}{2\sigma_y^2\psi_y^2} \right)$ ,  $A_{mod} = A_0 G$ , and  $\sigma_{mod}^2 = \left( \frac{3\mu_x^2\sigma_x^4 + 3\mu_y^2\sigma_y^4 + \sigma_x^6 + \sigma_y^6}{2} \right)^{\frac{1}{3}}$ ,  $\psi_{mod} = \frac{w_{zeq}}{2\sigma_{mod}}$  [4]. Further, we assume that  $E[s_i^2] = 1$ , where  $E[\cdot]$  is the expectation operator. Then, the total average received

signal-to-noise ratio (SNR) is given as  $\bar{\gamma} = \frac{\eta^2}{\sigma^2 N^2} E[(\sum_{i=1}^N v_i I_i)^2]$  and  $G_{p,q}^{m,n} \left( z \left| \begin{smallmatrix} a_1, \dots, a_p \\ b_1, \dots, b_q \end{smallmatrix} \right. \right)$  represents the Meijer-G function.

## 2.2 Decoding of Received Symbols

Let us consider the case of a  $2 \times 1$  FSO MISO system. Thus, in this case  $N = 2$ . The main technique used to decode individual symbol is interference cancellation (IC). There are two kinds of IC techniques: (i) pre-IC where IC is done at the TX side and (ii) post-IC where IC is done at RX side. A necessary condition for the pre-IC is to employ an optimum beamforming scheme at the TX side. For this, a steady information of CSI is required at the TX side which necessitates the existence of a feedback path from the RX to the TX side. On the other hand, for the post-IC technique, we use SIC to detect the symbol with the highest channel gain. Let us consider  $I_1 > I_2$ . Then,  $s_1$  will be estimated first considering  $s_2$  as noise. Let the estimated symbol be denoted by  $\hat{s}_1$  which is then subtracted from the received signal given in (1). This process will go on till each symbol is detected. If the symbol is estimated correctly, then there is no SIC error; otherwise, the SIC error is present. Thus, we have:

$$\hat{y} = \begin{cases} v_1 I_1 (s_1 - \hat{s}_1) + v_2 I_2 s_2 + e, & \text{SIC error present} \\ v_2 I_2 s_2 + e, & \text{SIC error absent} \end{cases} \quad (3)$$

Each symbol is estimated using maximum likelihood detection (MLD) from (3).

## 3. Computation of Average Bit Error Rate

In order to find the average bit error rate (ABER) of the considered system, the following two cases are considered:

Case 1: When  $I_1 > I_2$

In this case, the received signal at the RX is given by (1) and the symbols are detected using (3). The instantaneous BER for the case when  $I_1 > I_2$  for the symbol transmitted from the first antenna is given by:

$$P_e(TX_1 | I_1 > I_2) = \frac{1}{2} Q \left( \frac{\sqrt{\gamma}(v_1 I_1 + v_2 I_2)}{2} \right) + \frac{1}{2} Q \left( \frac{\sqrt{\gamma}(v_1 I_1 - v_2 I_2)}{2} \right), \quad (4)$$

where  $Q(\cdot)$  is the Gaussian  $Q$  function. Once  $s_1$  is detected, it will be modulated again and then subtracted as explained in (3). After this, two scenarios arise: (i) when  $s_1 = \hat{s}_1$  which represents the situation where no SIC error has occurred and (ii) when  $s_1 \neq \hat{s}_1$  which indicates that SIC error has occurred. The instantaneous BERs for these two scenarios, after simplification, are expressed as:

$$P_e(TX_2 | I_1 > I_2, s_1 = \hat{s}_1) = \left[ 1 - \frac{1}{2} Q \left( \frac{\sqrt{\gamma}(v_1 I_1 + v_2 I_2)}{2} \right) - \frac{1}{2} Q \left( \frac{\sqrt{\gamma}(v_1 I_1 - v_2 I_2)}{2} \right) \right] Q \left( \frac{\sqrt{\gamma} v_2 I_2}{2} \right), \quad (5)$$

$$P_e(TX_2|I_1 > I_2, s_1 \neq \hat{s}_1) = \left[ \frac{1}{2} Q \left( \frac{\sqrt{\gamma}(v_1 I_2 + 2v_2 I_1)}{2} \right) - \frac{1}{2} Q \left( \frac{\sqrt{\gamma}(v_2 I_1 - 2v_2 I_1)}{2} \right) \right] \left[ \frac{1}{2} Q \left( \frac{\sqrt{\gamma}(v_1 I_1 + v_2 I_2)}{2} \right) - \frac{1}{2} Q \left( \frac{\sqrt{\gamma}(v_1 I_1 - v_2 I_2)}{2} \right) \right]. \quad (6)$$

Case 2:  $I_2 > I_1$

Following an approach similar to the previous case, the instantaneous BERs for this scenario are given as:

$$P_e(TX_2|I_2 > I_1) = \frac{1}{2} Q \left( \frac{\sqrt{\gamma}(v_1 I_2 + v_2 I_1)}{2} \right) + \frac{1}{2} Q \left( \frac{\sqrt{\gamma}(v_1 I_2 - v_2 I_1)}{2} \right), \quad (7)$$

$$P_e(TX_1|I_2 > I_1, s_2 = \hat{s}_2) = \left[ 1 - \frac{1}{2} Q \left( \frac{\sqrt{\gamma}(v_1 I_2 + v_2 I_1)}{2} \right) - \frac{1}{2} Q \left( \frac{\sqrt{\gamma}(v_1 I_2 - v_2 I_1)}{2} \right) \right] Q \left( \frac{\sqrt{\gamma} v_2 I_1}{2} \right), \quad (8)$$

$$P_e(TX_1|I_2 > I_1, s_2 \neq \hat{s}_2) = \left[ \frac{1}{2} Q \left( \frac{\sqrt{\gamma}(v_1 I_1 + 2v_2 I_2)}{2} \right) - \frac{1}{2} Q \left( \frac{\sqrt{\gamma}(v_1 I_1 - 2v_2 I_2)}{2} \right) \right] \left[ \frac{1}{2} Q \left( \frac{\sqrt{\gamma}(v_1 I_2 + v_2 I_1)}{2} \right) - \frac{1}{2} Q \left( \frac{\sqrt{\gamma}(v_1 I_2 - v_2 I_1)}{2} \right) \right]. \quad (9)$$

Therefore, the overall ABER for the first TX is given by:

$$\bar{P}_e(TX_1) = \int_0^\infty \int_{I_2}^\infty P_e(TX_1|I_1 > I_2) f_{I_1}(I_1) f_{I_2}(I_2) dI_1 dI_2 + \int_0^\infty \int_{I_1}^\infty P_e(TX_1|I_2 > I_1, s_2 = \hat{s}_2) f_{I_1}(I_1) f_{I_2}(I_2) dI_2 dI_1 + \int_0^\infty \int_{I_1}^\infty P_e(TX_1|I_2 > I_1, s_2 \neq \hat{s}_2) f_{I_1}(I_1) f_{I_2}(I_2) dI_1 dI_2, \quad (10)$$

where  $f_{I_i}(I_i)$  is given by (2). Similarly, the ABER for the 2<sup>nd</sup> TX is expressed as:

$$\bar{P}_e(TX_2) = \int_0^\infty \int_{I_1}^\infty P_e(TX_2|I_2 > I_1) f_{I_1}(I_1) f_{I_2}(I_2) dI_2 dI_1 + \int_0^\infty \int_{I_2}^\infty P_e(TX_2|I_1 > I_2, s_1 = \hat{s}_1) f_{I_1}(I_1) f_{I_2}(I_2) dI_1 dI_2 + \int_0^\infty \int_{I_2}^\infty P_e(TX_2|I_1 > I_2, s_1 \neq \hat{s}_1) f_{I_1}(I_1) f_{I_2}(I_2) dI_1 dI_2. \quad (11)$$

The closed-form expressions for (10) and (11) can be obtained following the approach in [2].

## 5. Numerical Results

In this section, we discuss the average BER versus SNR performance of the considered FSO-NOMA system for  $N \in \{2, 3, 4\}$ . We consider strong and weak turbulence for  $\mathcal{M}$  distribution with parameters  $\{\alpha = 2.296, \beta = 2\}$  and  $\{\alpha = 8, \beta = 4\}$ , respectively. The other parameters considered are link length  $L = 1$  km, operational wavelength  $\lambda = 1550$  nm,  $b_0 = 0.1079$ ,  $\Omega = 1.3265$ ,  $\rho = 0.596$ , and  $\phi_a - \phi_b = \frac{\pi}{2}[2, 3]$ . The boresight PE parameters are chosen as  $\{\frac{\mu_x}{a} = 1, \frac{\mu_y}{a} = 2\}$  with jitter  $\{\frac{\sigma_x}{a} = 4, \frac{\sigma_y}{a} = 3\}$ . We observe from Fig. 1 that as we move from strong to weak turbulence regime, the average BER performance improves. It is also inferred that the high BER performance even in the weak turbulence regime is due to the presence of the combined effects of boresight and SIC errors.

Furthermore, as the number of TXs increases, the number of different symbols being transmitted in the same time and frequency domain also increases. Thus, the performance of the

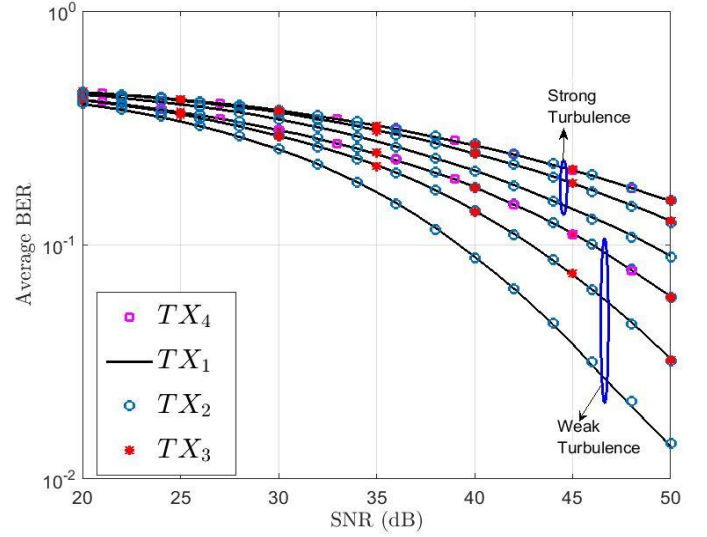


Fig. 1. Performance comparison of  $N \times 1$  FSO NOMA system with  $N = 2, 3, 4$  for weak and strong turbulence with non-zero boresight pointing error

systems deteriorates. Moreover, it can be seen that despite the increase in the number of TXs, the performance of all the TXs is identical. This is because allotting a higher beamforming weight to the TX with a higher channel gain and slightly lower beamforming weights to the other TXs in the decreasing order increases the difference in the received power level of each TX. This, in turn, helps to perform a successful SIC which mitigates the SIC error that occurs in a typical NOMA system.

## 6. Acknowledgement

This research was supported by the Basic Science Research Program through the National Research Foundation of Korea (NRF) funded by the Ministry of Education (2018R1D1A3B07049858).

## 7. Conflict of interest

The authors declare that there is no conflict of interest in this paper.

## 8. References

- [1] M. Z. Chowdhury, M. Shahjalal, S. Ahmed and Y. M. Jang, "6G Wireless Communication Systems: Applications, Requirements, Technologies, Challenges, and Research Directions," in *IEEE Open Journal of the Commun. Soc.*, vol. (2020) 957-975.
- [2] P. Saxena and M. R. Bhatnagar, "1-bit feedback-based beamforming scheme for an uplink FSO-NOMA system with SIC errors," *Appl. Opt.* 59, (2020) 11274-11291.
- [3] P. Saxena, A. Mathur, M. R. Bhatnagar and Z. Ghassemlooy, "BER of an optically pre-amplified FSO system under Málaga turbulence, pointing errors, and ASE noise," 2017 IEEE 28th Annual International Symposium on Personal, Indoor, and Mobile Radio Communications (PIMRC), (2017), 1-6
- [4] G. D. Verma, A. Mathur, Y. Ai, M. Cheffena, "Secrecy performance of FSO communication systems with non-zero boresight pointing errors," *IET Commun.*, (2021), 155-162